

LuMon: A Comprehensive Benchmark and Development Suite with Novel Datasets for Lunar Monocular Depth Estimation

Supplementary Material

A. Evaluation Metrics

To quantitatively evaluate the depth prediction performance against the ground truth, we utilize a standard set of depth estimation metrics [8]. Let N be the total number of valid pixels in the evaluation set, d_i denote the predicted depth at pixel i , and d_i^* denote the corresponding ground-truth depth.

Threshold Accuracy (δ_n): This metric measures the percentage of pixels where the relative error between the predicted and ground-truth depth falls within a specified threshold. Higher values indicate better performance.

$$\delta_n = \frac{1}{N} \sum_{i=1}^N \mathbf{1} \left(\max \left(\frac{d_i}{d_i^*}, \frac{d_i^*}{d_i} \right) < 1.25^n \right) \quad (\text{S1})$$

where $n \in \{1, 2, 3\}$ and $\mathbf{1}(\cdot)$ is the indicator function.

Absolute Relative Error (A.Rel): This computes the mean of the absolute percentage errors across all valid pixels.

$$\text{A.Rel} = \frac{1}{N} \sum_{i=1}^N \frac{|d_i - d_i^*|}{d_i^*} \quad (\text{S2})$$

Squared Relative Error (Sq.Rel): Similar to A.Rel, but the relative differences are squared, which more heavily penalizes large errors.

$$\text{Sq.Rel} = \frac{1}{N} \sum_{i=1}^N \frac{(d_i - d_i^*)^2}{d_i^*} \quad (\text{S3})$$

Root Mean Square Error (RMSE): A standard statistical metric that measures the root of the average squared difference, capturing the magnitude of the error in the original metric space.

$$\text{RMSE} = \sqrt{\frac{1}{N} \sum_{i=1}^N (d_i - d_i^*)^2} \quad (\text{S4})$$

Mean Absolute Error (MAE): The simple average of the absolute differences between the predicted and ground-truth depth values.

$$\text{MAE} = \frac{1}{N} \sum_{i=1}^N |d_i - d_i^*| \quad (\text{S5})$$

Scale-Invariant Logarithmic Error (SILog): This metric evaluates the error independently of the global scale, focusing strictly on the quality of the relative depth structures.

$$\text{SILog} = \frac{1}{N} \sum_{i=1}^N (\log d_i - \log d_i^*)^2 - \frac{1}{N^2} \left(\sum_{i=1}^N (\log d_i - \log d_i^*) \right)^2 \quad (\text{S6})$$

Edge Metrics (E.Acc and E.Comp): To evaluate the structural fidelity at depth boundaries, we employ the edge accuracy (Acc-Edges) and edge completion (Comp-Edges) metrics from the IBims-1 benchmark [25]. These metrics isolate depth boundary pixels identified via edge detection on the log-depth maps. Let E_p be the set of spatial pixel coordinates representing edges in the predicted depth map, and E_{gt} be the set of spatial pixel coordinates for edges in the ground-truth depth map.

Edge Accuracy (E_{acc}) measures the precision of the predicted depth discontinuities by computing the average distance from each predicted edge pixel to its nearest ground-truth counterpart:

$$E_{acc} = \frac{1}{|E_p|} \sum_{x \in E_p} \min \left(\min_{y \in E_{gt}} \|x - y\|_2, \theta \right) \quad (S7)$$

Edge Completion (E_{comp}) measures the recall, effectively evaluating how well the model maintains the sharpness of edges compared to the ground truth by computing the average distance from each ground-truth edge pixel to the nearest predicted edge:

$$E_{comp} = \frac{1}{|E_{gt}|} \sum_{y \in E_{gt}} \min \left(\min_{x \in E_p} \|x - y\|_2, \theta \right) \quad (S8)$$

where $|E|$ denotes the total number of pixels in the respective edge set, $\|x - y\|_2$ represents the Euclidean distance between two pixel coordinates, and θ is a maximum distance threshold (typically $\theta = 10$ pixels) used to cap the penalty for extreme outliers. For both metrics, a lower value indicates better structural fidelity at depth boundaries.

Median Translation Error: Let R and \hat{R} denote the ground-truth and estimated relative rotation matrices between two views. The rotation error is defined as the geodesic distance between the two rotations:

$$\epsilon_R = \arccos \left(\frac{\text{Tr} \left(R^\top \hat{R} \right) - 1}{2} \right) \quad (S9)$$

where $\text{Tr}(\cdot)$ denotes the matrix trace. The median rotation error is computed across all evaluated image pairs.

Median Translation Error: Let t and \hat{t} denote the ground-truth and estimated relative translation vectors. We measure the angular error between the translation directions:

$$\epsilon_t = \arccos \left(\frac{t^\top \hat{t}}{\|t\| \|\hat{t}\|} \right) \quad (S10)$$

The median translation error is then computed over all image pairs.

Area Under Curve: We evaluate the overall pose accuracy using the Area Under the Curve (AUC) of the pose error distribution. For each image pair, the pose error is defined as

$$\epsilon = \max(\epsilon_R, \epsilon_t). \quad (S11)$$

The AUC is computed as the area under the cumulative accuracy curve up to a threshold τ :

$$\text{AUC@}\tau = \frac{1}{\tau} \int_0^\tau A(e) de \quad (S12)$$

where $A(e)$ denotes the fraction of image pairs whose pose error ϵ is smaller than e . We report AUC values for $\tau \in \{5^\circ, 10^\circ, 20^\circ\}$.

B. Relative Pose Estimation

Given two RGB images I_1 and I_2 , we first compute dense 2D pixel correspondences using the fast reciprocal matching procedure of MAST3R [26]:

$$p_{12}, p_{21} = \text{MAST3R}(I_1, I_2) \quad (S13)$$

where p_{12} and p_{21} denote the sets of matched pixel coordinates (u, v) from I_1 to I_2 and from I_2 to I_1 , respectively. Then, we extract pixel-wise depth maps D_1, D_2 using an MDE network:

$$D_i = \text{MDE_Model}(I_i), \quad i \in \{1, 2\}. \quad (S14)$$

The resulting depth maps D_1, D_2 and pixel correspondences p_{12}, p_{21} are then provided to the MADPose framework [50]. Given that both images share the same intrinsic calibration matrix K , we employ the calibrated solver of MADPose to estimate the relative camera pose between I_1 and I_2 .

C. Detailed Fine-Tuning Protocol for Sim-to-Real Adaptation (Exp. 5)

We fine-tune the *DepthAnything v2 metric-outdoor (ViT-L)* checkpoint on LuSNAR depth supervision using a decoder-focused LoRA setup. Starting from the full model ($\sim 335.3\text{M}$ trainable parameters under full fine-tuning), we freeze the pretrained encoder backbone and inject LoRA adapters into encoder linear projections while keeping the depth decoder trainable. With LoRA rank $r = 8$, scaling $\alpha = 16$, and dropout 0.0, this reduces trainable parameters to 34,092,737 ($\approx 34.1\text{M}$), while preserving strong adaptation capacity.

Data split and preprocessing. LuSNAR sequence splits are fixed as:

$$\mathcal{S}_{train} = \{\text{Moon_2, Moon_3, Moon_4, Moon_5, Moon_7, Moon_9}\},$$

$$\mathcal{S}_{val} = \{\text{Moon_6}\}, \quad \mathcal{S}_{test} = \{\text{Moon_1, Moon_8}\}.$$

RGB frames are normalized with ImageNet statistics, and image/depth pairs are resized with aspect-ratio preservation to input size 518 (rounded to a multiple of 14 for backbone compatibility). Depth validity masking removes non-finite values, non-positive depths, and invalid sentinel values (65504); for training/evaluation loss we further restrict to $d \leq 50$ m.

Objective function. Let M denote valid pixels in a sample, y_i the ground-truth depth, and \hat{y}_i the prediction. The total training loss is

$$\mathcal{L} = \lambda_s \mathcal{L}_{\text{SiLog}} + \lambda_g \mathcal{L}_{\nabla},$$

with $\lambda_s = \lambda_g = 1$. For scale-invariant logarithmic loss, we define

$$\delta_i = \log(y_i + \epsilon) - \log(\hat{y}_i + \epsilon),$$

$$\mathcal{L}_{\text{SiLog}} = \sqrt{\frac{1}{|M|} \sum_{i \in M} \delta_i^2 - \lambda \left(\frac{1}{|M|} \sum_{i \in M} \delta_i \right)^2} + \epsilon,$$

where $\lambda = 0.5$ and $\epsilon = 10^{-6}$. We complement this with a gradient-matching term over valid horizontal/vertical depth differences:

$$\mathcal{L}_{\nabla} = \frac{1}{2} \left(\text{mean}_{(i,j) \in M_x} |(\partial_x \hat{y})_{ij} - (\partial_x y)_{ij}| + \text{mean}_{(i,j) \in M_y} |(\partial_y \hat{y})_{ij} - (\partial_y y)_{ij}| \right).$$

Optimization details. We optimize trainable parameters with AdamW (learning rate 5×10^{-5} , weight decay 10^{-2}); total epochs are set to 80 with linear warm-up for 2 epochs followed by cosine decay to 10^{-6} . Batch size is selected automatically by OOM-safe probing (search range 128 \rightarrow 2), resulting in effective batch size 16 in the reported LoRA- $r = 8$ run. Early stopping uses validation AbsRel with patience 10; checkpoint selection is based on best validation AbsRel.

Evaluation protocol during training. For monitoring, we report $\delta_1, \delta_2, \delta_3$, MAE, AbsRel, RMSE, SiLog, SqRel, EdgeAcc and EdgeComp. Predictions are least-squares aligned to GT before metric computation, and the same 50 m validity mask is applied. Best-model selection is then used for the test-time results discussed in the main paper.

Table S1. Exp. 1: Results on **LunarSim** dataset. **Red** indicates the best result and **blue** indicates the second best.

Type	Method	$\delta_1 \uparrow$	$\delta_2 \uparrow$	$\delta_3 \uparrow$	A.Rel \downarrow	Sq.Rel \downarrow	RMSE \downarrow	MAE \downarrow	SILog \downarrow	E.Acc \downarrow	E.Comp \downarrow
Metric	DAv2-FT	0.84	0.97	0.99	0.13	2.04	13.96	7.04	15.95	2.56	130.43
	DepthAnything v2 [49]	0.56	0.81	0.89	0.26	3.62	15.18	10.04	95.84	3.57	106.37
	DepthAnything 3 [11]	0.63	0.85	0.91	0.22	2.84	14.15	8.89	55.14	3.19	157.79
	MoGe-2 [44]	0.77	0.93	0.97	0.15	1.76	12.17	6.80	24.89	2.02	140.01
	Depth Pro [4]	0.50	0.79	0.88	0.29	4.64	17.57	11.45	84.24	3.58	152.95
	Metric-3D v2 [19]	0.75	0.91	0.97	0.16	1.99	12.53	7.10	29.10	2.47	72.61
	UniDepth v2 [33]	0.76	0.90	0.95	0.21	5.12	16.16	8.89	23.48	1.98	168.42
	MapAnything [23]	0.87	0.97	0.99	0.11	1.23	10.74	5.53	25.10	2.42	169.53
	VDA [10]	0.75	0.93	0.98	0.16	2.23	13.94	7.41	25.10	2.51	96.24
	Metric Anything [9]	0.79	0.93	0.97	0.15	1.71	12.08	6.68	28.04	2.25	129.25
Relative	DepthAnything-AC [40]	0.70	0.85	0.91	0.28	8.12	19.12	11.43	26.00	2.36	152.78
	DepthCrafter [20]	0.40	0.73	0.81	0.37	6.62	20.28	14.05	316.46	4.39	208.08
	Lotus [17]	0.59	0.84	0.93	0.27	5.70	20.43	11.67	36.21	2.85	97.52
	MiDaS v3.1 [3]	0.78	0.95	0.99	0.17	2.68	14.97	7.85	20.56	2.60	147.71
	Marigold [22]	0.67	0.89	0.96	0.21	3.73	17.25	9.88	37.98	2.84	49.23

D. Extended Quantitative Results

D.1. Overall Evaluation

Tables S1 to S6 present the disaggregated per-dataset results that underpin the main text’s overall comparison (Exp. 1). While the main paper reports aggregated trends, here we provide the full metric breakdown for each benchmark individually to enable fine-grained analysis of cross-domain generalization patterns. Our affine-aligned evaluation protocol ensures that all comparisons, including those involving relative methods, reflect geometric and structural accuracy rather than raw scale recovery.

LunarSim (Tab. S1). On this synthetic benchmark, MapAnything achieves the strongest zero-shot performance among metric methods ($\delta_1=0.87$, A.Rel=0.11, RMSE=10.74), followed by DAv2-FT ($\delta_1=0.84$) and Metric Anything (RMSE=12.08). Among relative methods, MiDaS v3.1 attains the highest accuracy ($\delta_1=0.78$), yet remains behind the metric leaders. This gap indicates that metric foundation models encode stronger geometric priors that transfer more robustly to synthetic lunar terrain, even without domain-specific finetuning.

Table S2. Exp. 1: Results on **LuSNAR** dataset. **Red** indicates the best result and **blue** indicates the second best.

Type	Method	$\delta_1 \uparrow$	$\delta_2 \uparrow$	$\delta_3 \uparrow$	A.Rel \downarrow	Sq.Rel \downarrow	RMSE \downarrow	MAE \downarrow	SILog \downarrow	E.Acc \downarrow	E.Comp \downarrow
Metric	DAv2-FT	0.93	0.99	1.00	0.07	0.07	1.07	0.41	9.13	1.09	2.53
	DepthAnything v2 [49]	0.31	0.63	0.73	0.45	0.92	2.89	1.77	342.41	7.10	86.42
	DepthAnything 3 [11]	0.53	0.76	0.85	0.29	0.44	1.99	1.13	121.12	2.26	38.61
	MoGe-2 [44]	0.53	0.75	0.84	0.29	0.40	1.80	1.07	136.76	2.11	36.22
	Depth Pro [4]	0.33	0.64	0.72	0.45	0.91	2.70	1.69	374.12	6.65	99.65
	Metric-3D v2 [19]	0.61	0.79	0.86	0.25	0.33	1.71	0.97	108.62	1.92	45.65
	UniDepth v2 [33]	0.63	0.81	0.88	0.26	0.50	2.14	1.04	75.96	1.27	24.04
	MapAnything [23]	0.74	0.89	0.94	0.17	0.23	1.53	0.73	66.28	2.28	50.17
	VDA [10]	0.77	0.93	0.97	0.17	0.29	2.05	0.80	28.94	1.21	10.25
	Metric Anything [9]	0.51	0.74	0.83	0.30	0.41	1.83	1.11	136.98	1.82	48.57
Relative	DepthAnything-AC [40]	0.70	0.86	0.92	0.26	0.77	2.63	1.14	24.30	1.29	8.31
	DepthCrafter [20]	0.41	0.69	0.78	0.47	1.13	2.96	1.77	448.40	6.53	146.50
	Lotus [17]	0.36	0.70	0.85	0.44	1.05	3.08	1.71	150.41	2.82	35.69
	MiDaS v3.1 [3]	0.81	0.95	0.98	0.13	0.18	1.68	0.69	17.61	1.32	4.63
	Marigold [22]	0.62	0.81	0.87	0.24	0.36	2.02	1.03	72.64	1.79	12.26

LuSNAR (Tab. S2). The finetuned DAv2-FT model dominates across every metric ($\delta_1=0.93$, A.Rel=0.07, RMSE=1.07), establishing the upper bound on this dataset with a substantial margin over the second-best method, MiDaS v3.1 ($\delta_1=0.81$, RMSE=1.68). This result quantifies the direct benefit of domain-specific adaptation on synthetic lunar terrain. However, as discussed in Exp. 5 of the main text, this accuracy advantage does not transfer reliably to real-world imagery, underscoring the sim-to-real bottleneck that persists even after targeted finetuning.

Table S3. Exp. 1: Results on **Etna-LRNT** dataset. **Red** indicates the best result and **blue** indicates the second best.

Type	Method	$\delta_1 \uparrow$	$\delta_2 \uparrow$	$\delta_3 \uparrow$	A.Rel \downarrow	Sq.Rel \downarrow	RMSE \downarrow	MAE \downarrow	SILog \downarrow	E.Acc \downarrow	E.Comp \downarrow
Metric	DAv2-FT	1.00	1.00	1.00	0.05	0.01	0.13	0.10	5.56	1.90	41.06
	DepthAnything v2 [49]	1.00	1.00	1.00	0.06	0.01	0.15	0.12	7.01	3.81	4.84
	DepthAnything 3 [11]	1.00	1.00	1.00	0.04	0.01	0.11	0.08	4.91	2.39	36.57
	MoGe-2 [44]	0.99	1.00	1.00	0.05	0.01	0.16	0.11	6.37	3.33	13.87
	Depth Pro [4]	0.73	0.93	0.95	241.71	2415143.42	450.05	449.98	18.12	3.01	70.35
	Metric-3D v2 [19]	1.00	1.00	1.00	0.04	0.00	0.10	0.07	4.40	2.44	6.42
	UniDepth v2 [33]	1.00	1.00	1.00	0.03	0.00	0.07	0.05	3.12	1.73	15.91
	MapAnything [23]	1.00	1.00	1.00	0.03	0.00	0.08	0.06	3.26	1.73	19.73
	VDA [10]	1.00	1.00	1.00	0.04	0.01	0.12	0.08	4.90	1.91	10.24
	Metric Anything [9]	0.98	1.00	1.00	0.07	0.02	0.22	0.15	8.69	3.45	6.31
Relative	DepthAnything-AC [40]	1.00	1.00	1.00	0.05	0.01	0.12	0.10	5.76	1.66	62.56
	DepthCrafter [20]	0.92	0.99	1.00	0.10	0.03	0.27	0.20	12.71	4.21	21.02
	Lotus [17]	0.65	0.96	0.99	0.19	0.11	0.49	0.38	22.54	4.16	9.65
	MiDaS v3.1 [3]	1.00	1.00	1.00	0.04	0.01	0.12	0.09	5.37	1.68	77.97
	Marigold [22]	0.94	1.00	1.00	0.10	0.03	0.27	0.20	11.91	3.75	4.42

Etna-LRNT (Tab. S3). This Earth-based analog proves to be the least challenging benchmark, with nine methods reaching $\delta_1=1.00$. Because the well-lit volcanic terrain closely overlaps with standard terrestrial training distributions, the dataset cannot meaningfully differentiate model capabilities at the δ_1 level. Discrimination requires finer error metrics: UniDepth v2 and MapAnything both achieve A.Rel=0.03, with UniDepth v2 obtaining the lowest RMSE of 0.07 and SILog of 3.12. These results reinforce our main text observation that near-perfect performance on well-lit Earth analogs can be deceptive for evaluating mission-critical extraterrestrial deployment.

Table S4. Exp. 1: Results on **Etna-S3LI** dataset. **Red** indicates the best result and **blue** indicates the second best.

Type	Method	$\delta_1 \uparrow$	$\delta_2 \uparrow$	$\delta_3 \uparrow$	A.Rel \downarrow	Sq.Rel \downarrow	RMSE \downarrow	MAE \downarrow	SILog \downarrow
Metric	DAv2-FT	0.84	0.97	0.99	0.13	0.26	1.30	0.94	15.97
	DepthAnything v2 [49]	0.88	0.98	0.99	0.12	0.21	1.22	0.85	34.64
	DepthAnything 3 [11]	0.91	0.98	0.99	0.10	0.18	1.12	0.74	38.88
	MoGe-2 [44]	0.91	0.99	1.00	0.10	0.17	1.08	0.73	28.97
	Depth Pro [4]	0.89	0.98	1.00	0.11	0.18	1.11	0.78	16.58
	Metric-3D v2 [19]	0.87	0.98	0.99	0.12	0.22	1.19	0.83	27.04
	UniDepth v2 [33]	0.87	0.97	0.99	0.12	0.24	1.20	0.86	14.18
	MapAnything [23]	0.91	0.99	1.00	0.10	0.16	1.05	0.72	15.54
	VDA [10]	0.83	0.97	0.99	0.14	0.27	1.34	0.97	17.44
	Metric Anything [9]	0.91	0.99	1.00	0.10	0.16	1.05	0.72	17.23
Relative	DepthAnything-AC [40]	0.87	0.98	1.00	0.11	0.22	1.19	0.84	14.01
	DepthCrafter [20]	0.79	0.96	0.99	0.15	0.30	1.44	1.06	26.78
	Lotus [17]	0.80	0.96	0.99	0.15	0.31	1.45	1.05	20.62
	MiDaS v3.1 [3]	0.89	0.98	1.00	0.11	0.20	1.15	0.81	13.55
	Marigold [22]	0.86	0.97	0.99	0.12	0.24	1.26	0.89	22.09

Etna-S3LI (Tab. S4). The stricter LiDAR-derived ground truth of this dataset reveals tighter performance clustering among the top metric methods. Four architectures, namely DepthAnything 3, MoGe-2, MapAnything, and Metric Anything, tie at $\delta_1=0.91$ and A.Rel=0.10, with MapAnything and Metric Anything sharing the best RMSE of 1.05. MiDaS v3.1 is again the strongest relative method ($\delta_1=0.89$), narrowing the metric–relative gap relative to other benchmarks. This convergence indicates that when ground truth is calibrated via high-fidelity LiDAR rather than stereo reconstruction, the perceived advantage of metric models diminishes, suggesting that evaluation methodology itself significantly influences benchmark conclusions.

Table S5. Exp. 1: Results on **Chang’e-3** dataset. **Red** indicates the best result and **blue** indicates the second best.

Type	Method	$\delta_1 \uparrow$	$\delta_2 \uparrow$	$\delta_3 \uparrow$	A.Rel \downarrow	Sq.Rel \downarrow	RMSE \downarrow	MAE \downarrow	SILog \downarrow	E.Acc \downarrow	E.Comp \downarrow
Metric	DAv2-FT	0.92	1.00	1.00	0.08	0.08	0.70	0.51	10.45	3.34	401.86
	DepthAnything v2 [49]	0.95	1.00	1.00	0.06	0.05	0.56	0.41	8.30	3.42	71.96
	DepthAnything 3 [11]	0.96	1.00	1.00	0.05	0.03	0.44	0.30	7.77	3.00	242.66
	MoGe-2 [44]	0.95	1.00	1.00	0.06	0.04	0.45	0.32	7.40	2.76	126.03
	Depth Pro [4]	0.89	0.98	1.00	0.10	0.17	0.89	0.67	13.51	2.85	204.48
	Metric-3D v2 [19]	0.95	1.00	1.00	0.05	0.04	0.43	0.30	7.12	3.27	30.09
	UniDepth v2 [33]	0.94	1.00	1.00	0.07	0.05	0.54	0.39	8.53	3.50	93.81
	MapAnything [23]	0.95	1.00	1.00	0.07	0.05	0.52	0.37	9.32	3.85	130.95
	VDA [10]	0.93	1.00	1.00	0.08	0.07	0.68	0.48	10.22	3.72	185.00
	Metric Anything [9]	0.95	1.00	1.00	0.06	0.03	0.44	0.31	7.22	2.90	117.60
Relative	DepthAnything-AC [40]	0.66	0.90	0.99	0.22	0.43	1.55	1.25	22.98	3.79	529.25
	DepthCrafter [20]	0.86	0.99	1.00	0.13	0.16	1.05	0.84	16.20	3.32	323.26
	Lotus [17]	0.70	0.93	0.99	0.19	0.42	1.64	1.28	21.77	3.84	89.76
	MiDaS v3.1 [3]	0.81	0.96	1.00	0.15	0.22	1.12	0.88	16.89	4.15	392.09
	Marigold [22]	0.91	0.99	1.00	0.09	0.09	0.69	0.52	11.40	3.40	44.27

Chang’e-3 (Tab. S5). On authentic lunar surface imagery, metric foundation models demonstrate the strongest zero-shot transfer. DepthAnything 3 leads with $\delta_1=0.96$ and shares the best A.Rel of 0.05 with Metric-3D v2. Metric-3D v2 also achieves the lowest RMSE (0.43) and SILog (7.12), indicating superior absolute scale recovery on real extraterrestrial data. The consistently strong performance of metric architectures on this dataset validates their geometric priors for authentic lunar topography. Relative methods lag substantially; the best among them, Marigold, achieves only $\delta_1=0.91$ and RMSE=0.69, showing that affine-invariant representations sacrifice structural fidelity that is critical for mission-level accuracy.

Table S6. Exp. 1: Results on **CHERI** dataset. **Red** indicates the best result and **blue** indicates the second best.

Type	Method	$\delta_1 \uparrow$	$\delta_2 \uparrow$	$\delta_3 \uparrow$	A.Rel \downarrow	Sq.Rel \downarrow	RMSE \downarrow	MAE \downarrow	SILog \downarrow	E.Acc \downarrow	E.Comp \downarrow
Metric	DAv2-FT	0.36	0.70	0.84	0.50	2.55	3.90	3.31	50.74	2.46	84.84
	DepthAnything v2 [49]	0.32	0.65	0.83	0.54	2.88	4.14	3.56	50.62	3.23	94.51
	DepthAnything 3 [11]	0.34	0.69	0.85	0.51	2.63	3.97	3.39	48.38	2.65	69.40
	MoGe-2 [44]	0.32	0.65	0.83	0.54	2.84	4.12	3.54	50.92	3.24	174.46
	Depth Pro [4]	0.32	0.64	0.82	0.55	2.88	4.18	3.60	51.01	3.52	41.94
	Metric-3D v2 [19]	0.33	0.67	0.84	0.53	2.83	4.09	3.51	51.84	2.99	130.94
	UniDepth v2 [33]	0.35	0.69	0.85	0.51	2.69	3.99	3.40	50.05	2.78	136.55
	MapAnything [23]	0.36	0.71	0.85	0.50	2.62	3.91	3.31	48.24	3.69	221.03
	VDA [10]	0.43	0.76	0.87	0.44	2.18	3.56	2.94	55.49	2.40	144.99
	Metric Anything [9]	0.32	0.65	0.83	0.55	2.91	4.17	3.59	50.94	3.54	164.35
Relative	DepthAnything-AC [40]	0.54	0.83	0.91	0.35	1.60	3.09	2.42	98.96	1.67	75.36
	DepthCrafter [20]	0.33	0.64	0.83	0.53	2.75	4.08	3.52	50.40	5.21	74.63
	Lotus [17]	0.35	0.68	0.85	0.49	2.47	3.90	3.32	54.78	3.26	46.54
	MiDaS v3.1 [3]	0.40	0.74	0.86	0.46	2.35	3.71	3.10	52.27	2.39	97.14
	Marigold [22]	0.38	0.71	0.86	0.47	2.30	3.75	3.16	49.41	2.69	9.52

CHERI (Tab. S6). This dark analog benchmark represents the most challenging condition in our entire suite, where all methods suffer a severe performance collapse. The relative method DepthAnything-AC achieves the best results ($\delta_1=0.54$, A.Rel=0.35, RMSE=3.09), outperforming every metric-based approach. This constitutes a reversal of the dominant trend observed across all other benchmarks. The strongest metric method, VDA, reaches only $\delta_1=0.43$ and RMSE=3.56. This inversion suggests that the extreme high-contrast polar lighting conditions of CHERI severely disrupt the metric scaling learned from terrestrial data, whereas affine-invariant representations are inherently more resilient as they do not commit to an absolute depth scale. These findings show that illumination robustness remains a critical open challenge for deploying MDE models in harsh extraterrestrial lighting environments.

Table S7. Exp. 2: Results on **LunarSim** dataset (shaded regions). **Red** indicates the best result and **blue** indicates the second best.

Type	Method	$\delta_1\uparrow$	$\delta_2\uparrow$	$\delta_3\uparrow$	A.Rel \downarrow	Sq.Rel \downarrow	RMSE \downarrow	MAE \downarrow	SILog \downarrow	E.Acc \downarrow	E.Comp \downarrow
Metric	DAv2-FT	0.79	0.97	0.99	0.15	3.23	15.10	10.58	12.90	2.70	71.79
	DepthAnything v2 [49]	0.47	0.72	0.84	0.29	4.33	16.39	12.44	75.94	4.03	96.96
	DepthAnything 3 [11]	0.54	0.75	0.86	0.26	3.67	15.77	11.29	50.73	3.52	125.68
	MoGe-2 [44]	0.68	0.90	0.96	0.17	2.79	14.42	10.28	20.76	2.71	76.19
	Depth Pro [4]	0.38	0.62	0.75	0.35	6.84	21.33	15.72	91.85	4.09	116.75
	Metric-3D v2 [19]	0.62	0.85	0.94	0.20	3.11	14.35	9.59	25.92	3.32	41.03
	UniDepth v2 [33]	0.70	0.86	0.92	0.23	12.40	24.12	14.45	18.86	2.80	118.18
	MapAnything [23]	0.80	0.95	0.99	0.13	1.77	11.48	7.25	30.21	2.92	115.59
	VDA [10]	0.66	0.90	0.96	0.19	3.96	16.31	9.72	20.26	3.25	65.24
	Metric Anything [9]	0.74	0.92	0.96	0.16	2.39	13.19	9.40	24.83	2.99	65.14
Relative	DepthAnything-AC [40]	0.63	0.81	0.87	0.32	14.68	27.04	18.49	21.41	2.98	102.68
	DepthCrafter [20]	0.36	0.58	0.67	0.45	8.63	22.22	17.53	335.15	4.24	155.96
	Lotus [17]	0.46	0.77	0.91	0.32	12.83	29.36	19.24	27.68	3.23	64.85
	MiDaS v3.1 [3]	0.73	0.93	0.98	0.19	4.19	16.70	11.39	16.71	2.75	113.15
	Marigold [22]	0.51	0.79	0.90	0.29	7.52	21.92	16.57	36.53	3.05	44.39

D.2. Shaded Region Evaluation

Tables S7 to S12 report performance exclusively within shaded regions, extending the main text’s shadow analysis (Exp. 2) with full per-dataset breakdowns. In the absence of atmospheric scattering on the lunar surface, shadows exhibit near-zero illumination with razor-sharp boundaries, a condition fundamentally distinct from terrestrial shadow patterns. These tables quantify how each architecture handles this extreme loss of photometric information, which is essential for assessing safe autonomous navigation through permanently shadowed craters and polar terrain.

LunarSim (Tab. S7). MapAnything and DAv2-FT share the lead with $\delta_1=0.80$, though MapAnything achieves a lower A.Rel (0.13 vs. 0.15) and considerably better RMSE (11.48 vs. 15.10). Compared to the overall evaluation ($\delta_1=0.87$ for MapAnything), the degradation is moderate ($\Delta\delta_1\approx 0.07$), suggesting that the synthetic shading model preserves sufficient texture cues for the stronger architectures. Among relative methods, MiDaS v3.1 drops from $\delta_1=0.78$ to 0.73, indicating comparable resilience. This relatively mild degradation further suggests that synthetic shadow rendering, while useful for controlled evaluation, may underestimate the severity of real vacuum shadows.

Table S8. Exp. 2: Results on **LuSNAR** dataset (shaded regions). **Red** indicates the best result and **blue** indicates the second best.

Type	Method	$\delta_1 \uparrow$	$\delta_2 \uparrow$	$\delta_3 \uparrow$	A.Rel \downarrow	Sq.Rel \downarrow	RMSE \downarrow	MAE \downarrow	SILog \downarrow	E.Acc \downarrow	E.Comp \downarrow
Metric	DAv2-FT	0.84	0.96	1.00	0.11	0.10	0.95	0.49	7.94	1.57	27.25
	DepthAnything v2 [49]	0.20	0.37	0.45	0.66	1.39	2.86	2.11	407.91	7.59	62.95
	DepthAnything 3 [11]	0.34	0.54	0.68	0.40	0.64	2.15	1.39	131.02	3.50	42.53
	MoGe-2 [44]	0.35	0.53	0.65	0.41	0.59	1.90	1.31	147.67	3.34	44.50
	Depth Pro [4]	0.23	0.39	0.46	0.68	1.40	2.83	2.04	430.27	7.58	67.47
	Metric-3D v2 [19]	0.39	0.57	0.69	0.38	0.57	1.92	1.30	120.21	3.56	52.68
	UniDepth v2 [33]	0.45	0.67	0.79	0.36	1.12	2.85	1.43	78.12	2.65	51.20
	MapAnything [23]	0.60	0.81	0.90	0.22	0.32	1.64	0.95	65.72	2.67	51.88
	VDA [10]	0.65	0.88	0.96	0.23	0.50	2.19	1.17	22.18	2.04	41.74
	Metric Anything [9]	0.32	0.50	0.63	0.42	0.62	2.00	1.38	147.60	3.66	50.11
Relative	DepthAnything-AC [40]	0.54	0.76	0.87	0.38	1.95	3.80	1.73	22.53	2.24	47.40
	DepthCrafter [20]	0.28	0.44	0.52	0.81	2.16	3.17	2.28	523.05	7.91	70.24
	Lotus [17]	0.28	0.55	0.68	0.64	2.11	3.94	2.32	154.32	3.86	64.37
	MiDaS v3.1 [3]	0.64	0.89	0.95	0.20	0.45	1.99	1.19	16.60	2.12	45.19
	Marigold [22]	0.43	0.60	0.69	0.37	0.75	2.40	1.49	82.79	3.49	50.92

LuSNAR (Tab. S8). DAv2-FT maintains clear dominance ($\delta_1=0.84$, A.Rel=0.11, RMSE=0.95), benefiting from its explicit finetuning on LuSNAR geometry. The gap to the second-best method widens compared to the overall setting: VDA reaches only $\delta_1=0.65$, and MapAnything follows with RMSE=1.64. Among relative methods, MiDaS v3.1 ($\delta_1=0.64$, A.Rel=0.20) outperforms DepthAnything-AC, which drops sharply to $\delta_1=0.54$. The amplified performance gap under shading suggests that domain-adapted models internalize geometric structure more deeply than photometric appearance, whereas zero-shot models increasingly rely on surface texture that is absent in shadowed regions.

Table S9. Exp. 2: Results on **Etna-LRNT** dataset (shaded regions). **Red** indicates the best result and **blue** indicates the second best.

Type	Method	$\delta_1 \uparrow$	$\delta_2 \uparrow$	$\delta_3 \uparrow$	A.Rel \downarrow	Sq.Rel \downarrow	RMSE \downarrow	MAE \downarrow	SILog \downarrow	E.Acc \downarrow	E.Comp \downarrow
Metric	DAv2-FT	1.00	1.00	1.00	0.06	0.01	0.10	0.09	1.25	2.85	37.38
	DepthAnything v2 [49]	0.99	1.00	1.00	0.07	0.01	0.12	0.12	2.24	2.60	12.35
	DepthAnything 3 [11]	1.00	1.00	1.00	0.05	0.00	0.07	0.07	1.50	2.55	27.67
	MoGe-2 [44]	0.99	1.00	1.00	0.05	0.01	0.08	0.08	1.61	2.81	21.85
	Depth Pro [4]	0.39	0.83	0.92	559.37	5590194.98	818.97	818.96	4.29	4.19	34.97
	Metric-3D v2 [19]	1.00	1.00	1.00	0.05	0.00	0.07	0.07	1.51	2.69	23.61
	UniDepth v2 [33]	1.00	1.00	1.00	0.03	0.00	0.05	0.04	1.06	2.62	9.91
	MapAnything [23]	1.00	1.00	1.00	0.03	0.00	0.04	0.04	0.95	2.68	21.65
	VDA [10]	1.00	1.00	1.00	0.06	0.01	0.09	0.09	1.34	2.42	16.69
	Metric Anything [9]	0.99	1.00	1.00	0.07	0.01	0.12	0.11	2.12	2.80	15.29
Relative	DepthAnything-AC [40]	1.00	1.00	1.00	0.09	0.01	0.13	0.12	1.48	2.81	40.81
	DepthCrafter [20]	0.89	1.00	1.00	0.11	0.03	0.18	0.17	4.06	3.27	26.18
	Lotus [17]	0.45	0.87	1.00	0.29	0.17	0.42	0.41	5.76	2.89	9.48
	MiDaS v3.1 [3]	0.99	1.00	1.00	0.07	0.01	0.10	0.10	1.34	2.83	47.48
	Marigold [22]	0.90	1.00	1.00	0.11	0.03	0.17	0.16	3.15	2.62	8.27

Etna-LRNT (Tab. S9). Performance remains near-perfect for the leading methods, with six models attaining $\delta_1=1.00$. MapAnything and UniDepth v2 share the best A.Rel of 0.03, while MapAnything achieves the lowest RMSE (0.04). The controlled analog environment retains sufficient illumination variation for robust depth recovery even within shadows. As with the overall evaluation, the well-lit terrestrial nature of Etna-LRNT renders its shaded split too permissive to expose meaningful robustness differences, further confirming that this analog provides limited discriminative power for benchmarking extraterrestrial shadow handling.

Table S10. Exp. 2: Results on **Etna-S3LI** dataset (shaded regions). **Red** indicates the best result and **blue** indicates the second best.

Type	Method	$\delta_1 \uparrow$	$\delta_2 \uparrow$	$\delta_3 \uparrow$	A.Rel \downarrow	Sq.Rel \downarrow	RMSE \downarrow	MAE \downarrow	SILog \downarrow
Metric	DAv2-FT	0.46	0.70	0.84	0.29	1.14	2.88	2.59	15.79
	DepthAnything v2 [49]	0.47	0.63	0.68	0.43	2.36	3.54	3.27	109.25
	DepthAnything 3 [11]	0.53	0.65	0.68	0.46	2.90	3.58	3.30	80.69
	MoGe-2 [44]	0.56	0.69	0.73	0.38	2.30	3.22	2.92	95.08
	Depth Pro [4]	0.59	0.79	0.87	0.25	0.99	2.36	2.11	25.29
	Metric-3D v2 [19]	0.68	0.87	0.93	0.23	1.01	2.35	1.95	91.02
	UniDepth v2 [33]	0.75	0.93	0.98	0.17	0.65	1.90	1.66	10.68
	MapAnything [23]	0.80	0.95	0.98	0.15	0.47	1.63	1.40	9.75
	VDA [10]	0.48	0.71	0.85	0.28	0.99	2.61	2.34	14.30
	Metric Anything [9]	0.68	0.85	0.90	0.23	1.04	2.22	1.96	33.42
Relative	DepthAnything-AC [40]	0.62	0.90	0.97	0.20	0.63	2.13	1.87	11.47
	DepthCrafter [20]	0.46	0.67	0.75	0.38	1.93	3.33	3.02	62.79
	Lotus [17]	0.48	0.70	0.79	0.32	1.49	3.17	2.83	25.22
	MiDaS v3.1 [3]	0.79	0.95	0.99	0.15	0.49	1.75	1.52	9.79
	Marigold [22]	0.49	0.67	0.75	0.35	1.65	3.21	2.87	62.92

Etna-S3LI (Tab. S10). This dataset reveals a notable narrowing of the metric–relative gap under shading. MapAnything leads with $\delta_1=0.80$ and RMSE=1.63, but MiDaS v3.1 closely follows with $\delta_1=0.79$ and a matching A.Rel of 0.15. This convergence is significant: it suggests that when shadow-induced contrast loss eliminates the fine photometric details on which metric models rely for scale inference, relative methods, which are inherently scale-agnostic, can achieve competitive geometric accuracy. This observation has practical implications for mission planning in persistently shadowed regions, where relative depth estimation may offer a more robust fallback than metric architectures.

Table S11. Exp. 2: Results on **Chang’e-3** dataset (shaded regions). **Red** indicates the best result and **blue** indicates the second best.

Type	Method	$\delta_1 \uparrow$	$\delta_2 \uparrow$	$\delta_3 \uparrow$	A.Rel \downarrow	Sq.Rel \downarrow	RMSE \downarrow	MAE \downarrow	SILog \downarrow	E.Acc \downarrow	E.Comp \downarrow
Metric	DAv2-FT	0.89	0.99	1.00	0.10	0.10	0.73	0.55	10.59	3.74	241.28
	DepthAnything v2 [49]	0.94	1.00	1.00	0.07	0.06	0.59	0.44	8.36	3.43	50.51
	DepthAnything 3 [11]	0.94	1.00	1.00	0.06	0.04	0.45	0.32	9.67	3.09	119.34
	MoGe-2 [44]	0.93	1.00	1.00	0.07	0.05	0.46	0.34	7.81	2.71	95.83
	Depth Pro [4]	0.85	0.98	1.00	0.11	0.18	0.87	0.69	15.04	3.08	139.39
	Metric-3D v2 [19]	0.94	1.00	1.00	0.06	0.04	0.44	0.32	7.41	2.71	44.76
	UniDepth v2 [33]	0.92	1.00	1.00	0.08	0.06	0.54	0.41	8.75	3.12	115.59
	MapAnything [23]	0.93	1.00	1.00	0.08	0.06	0.55	0.40	13.22	3.58	187.74
	VDA [10]	0.90	1.00	1.00	0.10	0.09	0.68	0.51	10.33	3.67	176.46
	Metric Anything [9]	0.94	1.00	1.00	0.06	0.04	0.46	0.33	7.48	2.80	93.81
Relative	DepthAnything-AC [40]	0.58	0.85	0.98	0.26	0.58	1.68	1.34	21.47	4.64	417.57
	DepthCrafter [20]	0.83	0.97	0.99	0.14	0.20	1.11	0.87	15.25	4.03	256.90
	Lotus [17]	0.63	0.90	0.98	0.23	0.64	1.81	1.41	21.26	3.67	97.65
	MiDaS v3.1 [3]	0.74	0.94	1.00	0.18	0.27	1.17	0.93	16.48	4.41	404.92
	Marigold [22]	0.89	0.99	1.00	0.10	0.12	0.72	0.56	10.23	3.34	45.43

Chang’e-3 (Tab. S11). Four metric methods, DepthAnything v2, DepthAnything 3, Metric-3D v2, and Metric Anything, tie at $\delta_1=0.94$. Metric-3D v2 achieves the lowest RMSE (0.44) and DepthAnything 3 the lowest A.Rel (0.06). The shaded performance is remarkably close to the overall results, indicating that the authentic Chang’e-3 imagery, captured under the harsh, unfiltered solar illumination of the lunar surface, already inherently contains substantial high-contrast shadow content. Consequently, the shadow-masked split introduces minimal additional difficulty, and the per-method rankings remain largely consistent with the overall evaluation.

Table S12. Exp. 2: Results on **CHERI** dataset (shaded regions). **Red** indicates the best result and **blue** indicates the second best.

Type	Method	$\delta_1 \uparrow$	$\delta_2 \uparrow$	$\delta_3 \uparrow$	A.Rel \downarrow	Sq.Rel \downarrow	RMSE \downarrow	MAE \downarrow	SILog \downarrow	E.Acc \downarrow	E.Comp \downarrow
Metric	DAv2-FT	0.16	0.50	0.82	0.51	2.51	4.76	4.27	58.39	3.28	10.11
	DepthAnything v2 [49]	0.15	0.39	0.76	0.72	4.12	5.18	4.81	44.18	3.69	11.32
	DepthAnything 3 [11]	0.18	0.49	0.79	0.62	3.17	4.75	4.37	39.39	3.06	9.37
	MoGe-2 [44]	0.15	0.40	0.76	0.73	4.26	5.20	4.83	44.93	3.01	9.48
	Depth Pro [4]	0.13	0.45	0.73	0.78	4.73	5.27	4.93	47.67	3.46	9.83
	Metric-3D v2 [19]	0.16	0.43	0.78	0.68	3.83	5.06	4.67	46.47	2.88	11.23
	UniDepth v2 [33]	0.17	0.49	0.79	0.64	3.56	4.94	4.51	45.78	2.88	8.97
	MapAnything [23]	0.15	0.49	0.79	0.63	3.47	4.95	4.53	40.04	3.08	10.13
	VDA [10]	0.27	0.68	0.82	0.51	2.62	4.23	3.76	68.25	2.70	10.10
	Metric Anything [9]	0.14	0.40	0.75	0.74	4.33	5.24	4.88	45.18	2.98	11.05
Relative	DepthAnything-AC [40]	0.47	0.76	0.83	0.41	2.52	3.96	3.05	212.22	2.72	10.43
	DepthCrafter [20]	0.21	0.47	0.73	0.76	4.59	5.01	4.65	44.23	3.21	10.14
	Lotus [17]	0.21	0.53	0.79	0.58	3.18	4.71	4.22	92.98	2.91	5.01
	MiDaS v3.1 [3]	0.27	0.62	0.81	0.55	2.79	4.23	3.78	60.53	3.26	11.66
	Marigold [22]	0.18	0.47	0.81	0.51	2.40	4.65	4.20	53.26	2.83	6.37

CHERI (Tab. S12). This condition represents the hardest evaluation in our entire benchmark suite. DepthAnything-AC again leads ($\delta_1=0.47$, A.Rel=0.41, RMSE=3.96), though with degraded performance compared to its overall result ($\delta_1=0.54$). Metric methods deteriorate severely, with the best (VDA) reaching only $\delta_1=0.27$. The compounded difficulty of the dark analog terrain and deep shadows reduces many metric architectures to near-random performance, exposing a fundamental limitation: terrestrial metric priors, which implicitly encode assumptions about Earth-like illumination distributions, become unreliable under the extreme photometric conditions of polar and permanently shadowed lunar environments. Addressing this failure mode is essential for enabling safe autonomous navigation during future missions targeting the lunar south pole.

Table S13. Exp. 2: Results on **Regolith** regions on LuSNAR dataset. **Red** indicates the best result and **blue** indicates the second best.

Type	Method	$\delta_1 \uparrow$	$\delta_2 \uparrow$	$\delta_3 \uparrow$	A.Rel \downarrow	Sq.Rel \downarrow	RMSE \downarrow	MAE \downarrow	SILog \downarrow	E.Acc \downarrow	E.Comp \downarrow
Metric	DAv2-FT	0.93	0.99	1.00	0.07	0.04	0.75	0.30	8.59	0.34	2.92
	DepthAnything v2 [49]	0.30	0.61	0.71	0.46	0.84	2.24	1.52	350.76	7.34	104.45
	DepthAnything 3 [11]	0.52	0.75	0.84	0.29	0.40	1.63	0.99	123.58	1.98	44.95
	MoGe-2 [44]	0.52	0.74	0.83	0.30	0.38	1.53	0.97	139.21	2.51	39.42
	Depth Pro [4]	0.32	0.63	0.71	0.47	0.85	2.25	1.50	382.05	7.78	99.93
	Metric-3D v2 [19]	0.60	0.78	0.85	0.26	0.30	1.34	0.84	111.11	1.87	56.49
	UniDepth v2 [33]	0.62	0.81	0.88	0.27	0.40	1.40	0.86	76.29	1.23	26.64
	MapAnything [23]	0.73	0.89	0.94	0.17	0.19	1.14	0.61	62.38	1.37	15.17
	VDA [10]	0.77	0.93	0.97	0.17	0.17	1.11	0.59	28.88	0.73	5.82
	Metric Anything [9]	0.50	0.73	0.82	0.31	0.40	1.54	0.99	139.69	2.28	53.12
Relative	DepthAnything-AC [40]	0.69	0.86	0.92	0.27	0.61	1.54	0.87	22.25	0.39	4.22
	DepthCrafter [20]	0.40	0.68	0.77	0.48	1.08	2.41	1.55	458.01	7.77	145.34
	Lotus [17]	0.35	0.69	0.84	0.46	0.92	2.25	1.43	149.78	2.11	45.46
	MiDaS v3.1 [3]	0.81	0.96	0.98	0.13	0.12	1.19	0.53	17.02	0.51	4.15
	Marigold [22]	0.62	0.81	0.87	0.24	0.29	1.48	0.84	73.58	1.31	19.35

D.3. Semantic Region Evaluation

Tables S13 to S15 extend the main text’s topological analysis by providing the full per-method metric breakdown for each semantic surface category on LuSNAR: regolith, rock, and crater. For autonomous lunar rover navigation, accurate depth estimation over each terrain type is critical. Regolith constitutes the majority of traversable surface, rocks represent immediate collision hazards requiring reliable obstacle detection, and craters pose the most dangerous traversal risk due to their steep interior slopes and abrupt rim discontinuities. By leveraging the pixel-level semantic labels of LuSNAR, we isolate how well each architecture captures the distinct geometric characteristics of these geological constructs.

Regolith (Tab. S13). DAv2-FT achieves the best performance across all metrics ($\delta_1=0.93$, A.Rel=0.07, RMSE=0.75). MiDaS v3.1 is the strongest relative method ($\delta_1=0.81$, A.Rel=0.13). The relatively low error magnitudes across methods reflect the geometric simplicity of flat regolith surfaces, which lack the depth discontinuities and self-occlusion patterns that challenge monocular inference. From a deployment perspective, the consistently high accuracy on regolith is encouraging, as it confirms that current architectures can reliably estimate depth over the primary traversable terrain type.

Table S14. Exp. 2: Results on **Rocks** regions on LuSNAR dataset. **Red** indicates the best result and **blue** indicates the second best.

Type	Method	$\delta_1 \uparrow$	$\delta_2 \uparrow$	$\delta_3 \uparrow$	A.Rel \downarrow	Sq.Rel \downarrow	RMSE \downarrow	MAE \downarrow	SILog \downarrow	E.Acc \downarrow	E.Comp \downarrow
Metric	DAv2-FT	0.92	0.99	1.00	0.09	0.50	3.56	2.56	10.36	2.87	12.83
	DepthAnything v2 [49]	0.44	0.83	0.97	0.28	2.21	7.15	6.13	18.04	3.38	11.37
	DepthAnything 3 [11]	0.65	0.95	0.99	0.19	1.28	5.76	4.60	15.00	3.33	17.25
	MoGe-2 [44]	0.69	0.96	1.00	0.18	1.14	5.36	4.30	13.06	2.79	7.57
	Depth Pro [4]	0.45	0.83	0.96	0.28	2.46	7.49	6.41	18.03	2.66	6.00
	Metric-3D v2 [19]	0.80	0.97	0.99	0.15	1.00	4.76	3.70	12.87	3.16	9.12
	UniDepth v2 [33]	0.76	0.93	0.97	0.18	2.39	6.87	4.49	13.88	3.11	10.39
	MapAnything [23]	0.85	0.98	0.99	0.14	0.93	4.72	3.36	25.66	3.86	24.31
	VDA [10]	0.80	0.97	0.99	0.16	1.89	6.58	4.30	15.07	3.78	18.22
	Metric Anything [9]	0.67	0.96	1.00	0.18	1.14	5.33	4.33	13.30	2.82	8.12
Relative	DepthAnything-AC [40]	0.66	0.84	0.92	0.24	4.72	9.51	6.56	16.05	3.63	19.38
	DepthCrafter [20]	0.43	0.76	0.92	0.27	3.10	8.89	7.63	18.51	2.63	9.96
	Lotus [17]	0.51	0.79	0.91	0.28	5.25	10.30	7.55	21.30	3.45	14.99
	MiDaS v3.1 [3]	0.76	0.94	0.98	0.19	2.19	6.23	4.78	14.25	3.58	18.13
	Marigold [22]	0.66	0.94	0.99	0.21	1.76	6.06	4.83	15.19	3.21	10.19

Rock Regions (Tab. S14). Rocks introduce significantly greater difficulty. DAv2-FT remains the clear leader ($\delta_1=0.92$, A.Rel=0.09, RMSE=3.56), but the gap to the second-best method (MapAnything: $\delta_1=0.85$, RMSE=4.72) narrows compared to regolith. The elevated RMSE values across all methods, roughly $4\times$ larger than on regolith, indicate that the irregular geometry, sharp edges, and self-occlusion patterns of lunar boulders pose a tangible challenge even for finetuned models. Several zero-shot metric models (Metric-3D v2, MoGe-2) cluster around $\delta_1 \approx 0.74\text{--}0.78$, suggesting that generic terrestrial depth priors partially capture boulder-like geometry from their Earth-based training sets but fall short of the precision required for reliable obstacle avoidance during rover traverse planning.

Table S15. Exp. 2: Results on **Craters** regions on LuSNAR dataset. **Red** indicates the best result and **blue** indicates the second best.

Type	Method	$\delta_1\uparrow$	$\delta_2\uparrow$	$\delta_3\uparrow$	A.Rel \downarrow	Sq.Rel \downarrow	RMSE \downarrow	MAE \downarrow	SILog \downarrow	E.Acc \downarrow	E.Comp \downarrow
Metric	DAv2-FT	0.87	0.98	1.00	0.10	0.77	4.52	3.83	8.48	2.05	10.06
	DepthAnything v2 [49]	0.23	0.45	0.73	0.37	6.69	15.30	14.44	15.69	2.67	6.68
	DepthAnything 3 [11]	0.37	0.75	0.90	0.27	4.16	11.53	10.82	12.38	2.25	6.50
	MoGe-2 [44]	0.40	0.71	0.88	0.27	4.45	11.79	11.05	12.21	2.14	11.12
	Depth Pro [4]	0.23	0.44	0.72	0.37	7.14	15.72	14.82	15.87	2.29	5.56
	Metric-3D v2 [19]	0.41	0.75	0.90	0.27	3.87	11.11	10.31	19.84	2.46	9.85
	UniDepth v2 [33]	0.45	0.73	0.91	0.25	3.73	10.85	10.00	12.37	2.28	13.04
	MapAnything [23]	0.42	0.76	0.90	0.26	3.76	11.07	10.24	13.35	2.78	11.57
	VDA [10]	0.36	0.66	0.87	0.29	4.66	12.46	11.47	14.32	2.81	8.78
	Metric Anything [9]	0.41	0.73	0.88	0.27	4.42	11.60	10.93	11.99	2.19	10.07
Relative	DepthAnything-AC [40]	0.31	0.60	0.86	0.31	5.00	13.29	12.11	16.88	2.97	10.98
	DepthCrafter [20]	0.17	0.38	0.65	0.41	8.25	17.29	16.23	19.17	3.37	16.15
	Lotus [17]	0.21	0.47	0.68	0.39	7.22	15.50	14.38	19.93	3.66	13.84
	MiDaS v3.1 [3]	0.34	0.70	0.91	0.28	4.15	12.10	10.95	15.84	3.05	17.69
	Marigold [22]	0.26	0.58	0.80	0.33	5.70	14.11	12.98	17.45	3.24	7.93

Craters (Tab. S15). Craters constitute the hardest semantic category and expose the most severe performance cliff in our benchmark. While DAv2-FT achieves $\delta_1=0.87$, A.Rel=0.10, and RMSE=4.52, showing that targeted finetuning can meaningfully capture crater morphology, the second-best method, UniDepth v2, reaches only $\delta_1=0.45$ with an RMSE of 10.85, representing a $\sim 2.4\times$ error increase. This dramatic gap shows that crater geometry, with its sharp depth discontinuities at the rim, gradually varying concave interior slopes, and cast shadows, is extremely difficult for models without explicit lunar supervision. Craters represent the most hazardous terrain feature for rover navigation, and the near-total failure of zero-shot architectures to resolve their interior geometry underscores the necessity of domain-specific adaptation or physics-informed depth priors for safe autonomous traverse planning near crater boundaries.

Table S16. Exp. 3: Results on **Near (0–5m)** distances on LuSNAR dataset. **Red** indicates the best result and **blue** indicates the second best.

Type	Method	$\delta_1\uparrow$	$\delta_2\uparrow$	$\delta_3\uparrow$	A.Rel \downarrow	Sq.Rel \downarrow	RMSE \downarrow	MAE \downarrow	SILog \downarrow	E.Acc \downarrow	E.Comp \downarrow
Metric	DAv2-FT	0.92	0.98	1.00	0.07	0.02	0.16	0.14	6.96	0.41	7.46
	DepthAnything v2 [49]	0.30	0.55	0.64	0.49	0.68	1.13	0.99	379.83	7.18	158.41
	DepthAnything 3 [11]	0.48	0.69	0.80	0.31	0.31	0.70	0.61	130.89	2.85	84.58
	MoGe-2 [44]	0.48	0.68	0.78	0.32	0.31	0.70	0.62	148.40	3.24	102.99
	Depth Pro [4]	0.33	0.55	0.63	0.50	0.73	1.15	0.99	413.67	7.55	165.65
	Metric-3D v2 [19]	0.55	0.73	0.81	0.28	0.26	0.64	0.56	119.17	3.30	91.01
	UniDepth v2 [33]	0.57	0.76	0.85	0.30	0.38	0.66	0.59	79.06	2.07	57.54
	MapAnything [23]	0.71	0.87	0.92	0.18	0.14	0.41	0.35	64.98	1.62	33.76
	VDA [10]	0.74	0.91	0.96	0.19	0.14	0.43	0.37	28.28	0.95	15.13
	Metric Anything [9]	0.47	0.66	0.77	0.33	0.32	0.72	0.63	148.68	3.69	110.19
Relative	DepthAnything-AC [40]	0.66	0.83	0.91	0.31	0.61	0.66	0.61	17.25	0.61	14.86
	DepthCrafter [20]	0.42	0.64	0.71	0.52	0.96	1.25	1.00	500.38	7.46	163.07
	Lotus [17]	0.27	0.64	0.81	0.53	0.94	1.28	1.14	154.55	3.93	73.23
	MiDaS v3.1 [3]	0.79	0.95	0.98	0.14	0.07	0.33	0.28	15.01	0.69	21.74
	Marigold [22]	0.59	0.76	0.83	0.25	0.21	0.60	0.50	77.24	2.45	46.42

D.4. Distance-Stratified Evaluation

Tables S16 to S18 extend the main text’s distance analysis (Exp. 3) by providing the full metric breakdown for each depth interval on LuSNAR. The main paper established that metric and structurally constrained models preserve internal linearity; here, we present the detailed per-method results across three ranges, near (0–5 m), medium (5–15 m), and far (15–50 m), to expose how depth estimation quality degrades as a function of range. As discussed in Exp. 3, we apply a global least-squares affine alignment anchored by the dominant mid-range terrain, which allows us to interpret deviations in the near and far ranges as direct indicators of distance-dependent scale drift.

Near Range (0–5 m) (Tab. S16). DAv2-FT achieves outstanding accuracy ($\delta_1=0.92$, A.Rel=0.07, RMSE=0.16). MiDaS v3.1 is the best relative method ($\delta_1=0.79$, RMSE=0.33). While the low absolute RMSE values across all methods reflect the inherently small error magnitudes at short distances, relative errors (A.Rel) reveal meaningful performance differences. Several metric methods (DepthAnything v2, Depth Pro) exhibit A.Rel values exceeding 0.49, significantly worse than their mid-range performance. This near-field degradation, also observed in the main text for Chang’e-3 and CHERI, suggests that the global affine alignment, fitted primarily to the mid-range, cannot correct for non-linear distortions at close proximity, where scale drift is most pronounced for models that lack internal linearity.

Table S17. Exp. 3: Results on **Medium (5–15m)** distances on LuSNAR dataset. **Red** indicates the best result and **blue** indicates the second best.

Type	Method	$\delta_1\uparrow$	$\delta_2\uparrow$	$\delta_3\uparrow$	A.Rel \downarrow	Sq.Rel \downarrow	RMSE \downarrow	MAE \downarrow	SILog \downarrow	E.Acc \downarrow	E.Comp \downarrow
Metric	DAv2-FT	0.99	1.00	1.00	0.07	0.10	0.88	0.60	4.47	1.17	36.08
	DepthAnything v2 [49]	0.20	0.83	0.99	0.40	1.49	3.29	3.13	7.61	2.03	9.27
	DepthAnything 3 [11]	0.58	0.96	1.00	0.25	0.68	2.23	2.00	6.96	1.21	33.29
	MoGe-2 [44]	0.59	0.96	1.00	0.25	0.64	2.12	1.97	5.86	0.92	18.43
	Depth Pro [4]	0.19	0.87	0.99	0.39	1.44	3.21	3.05	7.35	1.31	26.11
	Metric-3D v2 [19]	0.74	0.98	1.00	0.19	0.45	1.77	1.53	8.70	1.34	13.91
	UniDepth v2 [33]	0.78	0.98	1.00	0.17	0.39	1.61	1.39	6.10	1.16	28.51
	MapAnything [23]	0.81	0.97	1.00	0.16	0.41	1.55	1.28	7.19	1.40	50.80
	VDA [10]	0.89	0.99	1.00	0.11	0.28	1.33	0.94	7.32	1.53	29.17
	Metric Anything [9]	0.56	0.96	1.00	0.26	0.68	2.22	2.06	5.79	0.99	21.98
Relative	DepthAnything-AC [40]	0.83	0.97	0.99	0.13	0.37	1.53	1.13	7.87	1.53	30.53
	DepthCrafter [20]	0.28	0.81	0.99	0.38	1.45	3.28	3.02	10.55	1.79	32.34
	Lotus [17]	0.64	0.92	0.99	0.19	0.49	1.99	1.58	14.25	2.22	10.18
	MiDaS v3.1 [3]	0.89	1.00	1.00	0.12	0.22	1.27	0.96	6.56	1.60	34.96
	Marigold [22]	0.66	0.97	1.00	0.21	0.53	2.01	1.71	8.49	2.11	8.47

Medium Range (5–15 m) (Tab. S17). As the implicit anchor range for our global affine alignment, the medium interval yields the highest overall accuracy. DAv2-FT reaches $\delta_1=0.99$ and A.Rel=0.07 with RMSE=0.88, approaching near-perfect performance. VDA and MiDaS v3.1 share the second-best δ_1 of 0.89, with MiDaS v3.1 achieving a slightly lower RMSE (1.27 vs. 1.33). The strong mid-range performance across a broad set of methods is consistent with the main text’s observation that models with adequate internal linearity recover well within the range that dominates the alignment fit. This serves as a useful baseline: deviations from this accuracy in the near and far ranges directly quantify the severity of each model’s scale drift.

Table S18. Exp. 3: Results on **Far (15–50m)** distances on LuSNAR dataset. **Red** indicates the best result and **blue** indicates the second best.

Type	Method	$\delta_1\uparrow$	$\delta_2\uparrow$	$\delta_3\uparrow$	A.Rel \downarrow	Sq.Rel \downarrow	RMSE \downarrow	MAE \downarrow	SILog \downarrow	E.Acc \downarrow	E.Comp \downarrow
Metric	DAv2-FT	0.93	0.99	0.99	0.09	0.49	3.70	2.60	11.91	1.52	11.10
	DepthAnything v2 [49]	0.60	0.85	0.95	0.20	2.28	8.78	6.50	25.11	2.77	14.19
	DepthAnything 3 [11]	0.75	0.93	0.98	0.16	1.31	6.27	4.59	19.20	1.96	41.20
	MoGe-2 [44]	0.82	0.96	0.99	0.13	0.97	5.57	3.91	16.50	1.13	20.87
	Depth Pro [4]	0.65	0.88	0.97	0.18	1.91	8.13	5.86	22.27	1.42	28.95
	Metric-3D v2 [19]	0.81	0.96	0.99	0.14	1.02	5.46	4.06	18.08	1.77	11.11
	UniDepth v2 [33]	0.76	0.92	0.96	0.15	1.82	6.85	4.53	16.10	1.63	36.02
	MapAnything [23]	0.85	0.97	0.99	0.12	0.86	5.02	3.51	32.38	3.02	74.35
	VDA [10]	0.76	0.94	0.99	0.16	1.62	6.83	4.58	19.16	2.73	58.16
	Metric Anything [9]	0.80	0.96	0.99	0.13	1.02	5.63	4.08	16.89	1.15	20.52
Relative	DepthAnything-AC [40]	0.66	0.83	0.90	0.21	3.12	8.75	6.06	19.86	2.29	27.67
	DepthCrafter [20]	0.57	0.84	0.95	0.21	2.31	8.90	6.62	24.53	1.80	40.18
	Lotus [17]	0.49	0.77	0.89	0.25	3.25	9.71	7.23	27.52	2.52	8.26
	MiDaS v3.1 [3]	0.79	0.94	0.98	0.14	1.19	5.77	4.10	18.24	2.15	33.28
	Marigold [22]	0.75	0.93	0.97	0.16	1.52	6.58	4.81	20.67	2.32	9.50

Far Range (15–50 m) (Tab. S18). DAv2-FT maintains its lead ($\delta_1=0.93$, A.Rel=0.09, RMSE=3.70), while MapAnything emerges as the second-best metric method ($\delta_1=0.85$, RMSE=5.02). The absolute RMSE values increase substantially across all methods compared to nearer ranges, as expected due to the larger physical depth magnitudes. Among relative methods, MiDaS v3.1 performs competitively ($\delta_1=0.79$, RMSE=5.77), yet the gap to the top metric methods widens compared to the medium range. This widening gap confirms that metric supervision provides a stronger inductive bias for recovering absolute scale at longer distances, where monocular depth cues grow increasingly ambiguous and the textureless lunar regolith offers minimal visual guidance. For autonomous rover navigation, reliable far-field depth estimation is critical for long-horizon path planning and hazard anticipation, and the present results show that it remains achievable primarily through domain-adapted or metrically supervised architectures.

D.5. Training Regime and Data Analysis

D.5.1. Training Scale

As illustrated in Fig. S1, we expand upon the main text’s observation that massive training scale cannot universally solve the lunar domain gap. By decomposing performance across specific conditions, we isolate exactly where data scaling succeeds and fails.

Overall and Shaded Performance: On the authentic Chang’e-3 dataset, increasing a model’s training scale strongly correlates with higher depth accuracy and reduced error. Crucially, this advantage holds steady even within heavily shaded regions. However, this trend does not generalize. On the challenging Cheri dark analog, scaling exhibits a reversed, non-significant trend, and it offers little to no consistent benefit across the synthetic benchmarks.

Distance-Dependent Scaling: When analyzing performance across depth ranges, we find that the benefits of scaling on Chang’e-3 are heavily localized to the near and medium fields. As the depth extends into the far range, the correlation weakens and loses strict statistical significance. This indicates that while massive terrestrial datasets help models extract nearby, high-frequency details, they provide diminishing returns for understanding distant, large-scale lunar topography.

Semantic Features: Finally, our evaluation of specific semantic regions within the LuSNAR dataset confirms that scale offers no statistically significant improvement for distinct geological constructs. The correlations for regolith, rocks, and craters all fall well short of significance. This reinforces a core takeaway: simply feeding a network more data does not inherently teach it to parse complex extraterrestrial geometries like craters and boulders.

D.5.2. Real Training Data

As illustrated in Fig. S2, we evaluate whether increasing the proportion of real-world terrestrial images in the training set improves lunar adaptation. Given the severe visual domain gap, relying on Earth-based priors yields largely negligible improvements.

Overall and Semantic Performance: Increasing the ratio of real training data shows no statistically significant correlation with depth accuracy or error reduction across the classic evaluations, extreme lighting conditions, or specific geological features such as regolith, rocks, and craters. Both the synthetic benchmarks and the authentic lunar analogs yield p -values well above the significance threshold. This indicates that simply injecting more terrestrial photography into the training pipeline does not resolve the broader lunar domain gap, nor does it improve the structural understanding of extraterrestrial obstacles.

Distance-Dependent Scaling: The distance-stratified evaluation reveals a highly isolated benefit: increasing the real data ratio correlates with reduced error strictly within the near-field range of the authentic Chang’e-3 imagery ($\rho = -0.677$, $p = 0.008$). However, this advantage entirely vanishes in the medium and far ranges, and critically, it does not generalize to any other dataset, including the Cheri analog. This lack of generalizability raises significant concerns regarding the use of terrestrial priors for space applications; while Earth-based textures might occasionally assist in resolving nearby, high-frequency surface details, they completely fail to supply the robust, transferrable geometric understanding required for safe and reliable lunar navigation.

D.5.3. Metric Supervision

As illustrated in Fig. S3, we conclude our data analysis by evaluating the influence of metric supervision. We investigate whether training with a higher percentage of absolute metric ground truth inherently translates to better zero-shot scale recovery and structural accuracy on the Moon.

Overall and Shaded Performance: Across both the classic evaluations and the extreme lighting scenarios, we observe a complete absence of statistical significance. For every dataset, including the synthetic environments, Earth analogs, and authentic Chang’e-3 imagery, the correlations between metric supervision and performance metrics (δ_1 , Abs Rel, RMSE) yield p -values well above the 0.05 threshold.

Semantic and Distance-Dependent Scaling: This lack of correlation persists even under granular inspection. Stratifying the evaluation by specific geological constructs (regolith, rocks, craters) or by distance intervals (near, medium, far) fails to reveal any localized advantages. Not a single p -value across these breakdowns approaches statistical significance.

Primary Takeaway: These universally unpromising results forcefully demonstrate that the raw volume of metric supervision does not guarantee cross-domain robustness. Models trained with near-total metric supervision perform no better in extraterrestrial environments than those relying on affine-invariant or mixed-supervision strategies. This heavily reinforces our overarching conclusion: resolving the lunar sim-to-real domain gap will require targeted architectural innovations—such as decoupling illumination or integrating physics-based priors—rather than simply scaling up metric datasets.

E. Additional Visualizations

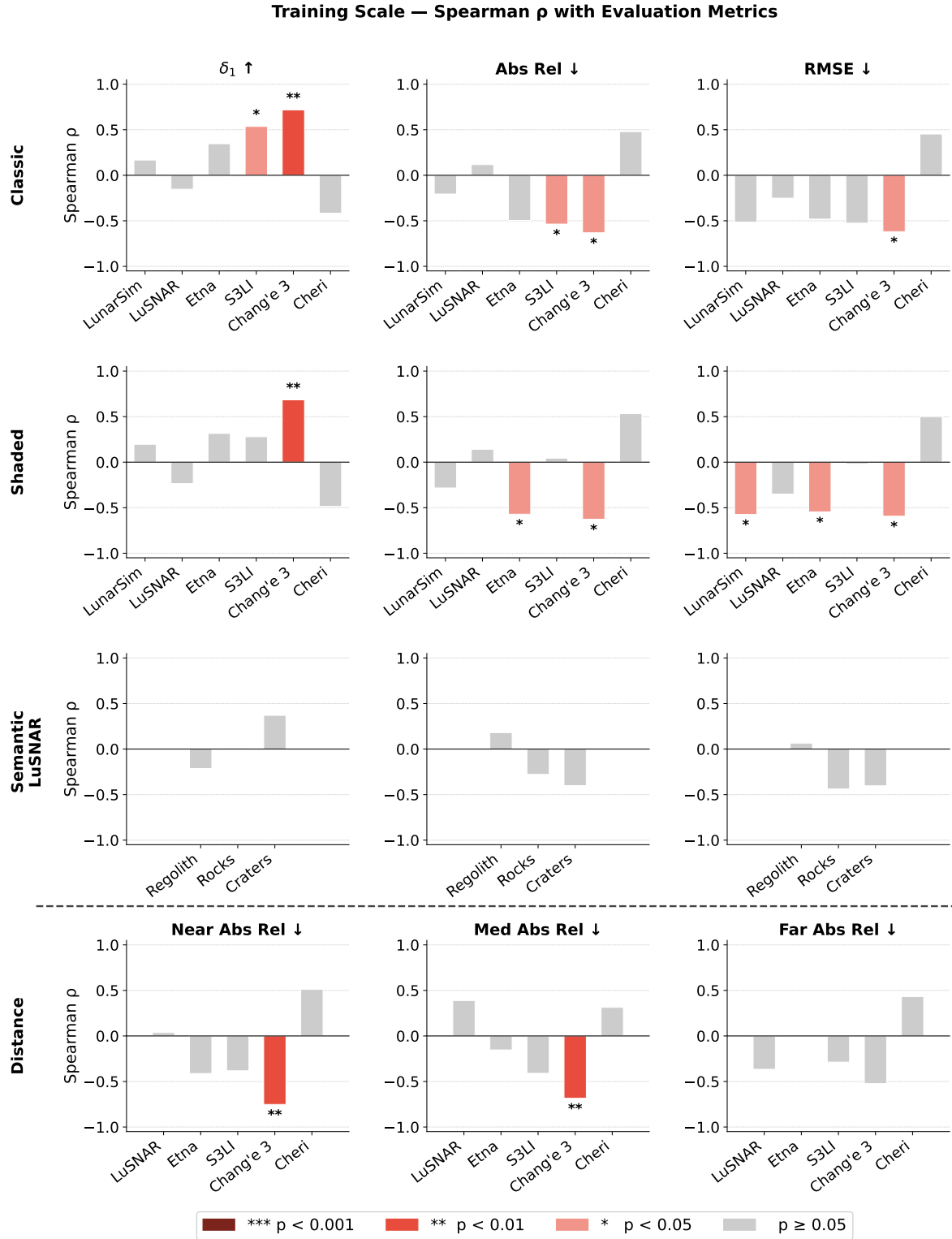


Figure S1. Spearman rank correlation (ρ) between model Training Scale and evaluation metrics. The figure illustrates the correlation of the models' total training scale with depth estimation performance (δ_1 , Abs Rel, RMSE) across standard dataset evaluations (Classic), extreme lighting conditions (Shaded), specific geological features (Semantic LuSNAR: Regolith, Rocks, Craters), and varying depth intervals (Distance: Near, Medium, Far). Statistical significance is indicated by p-values.

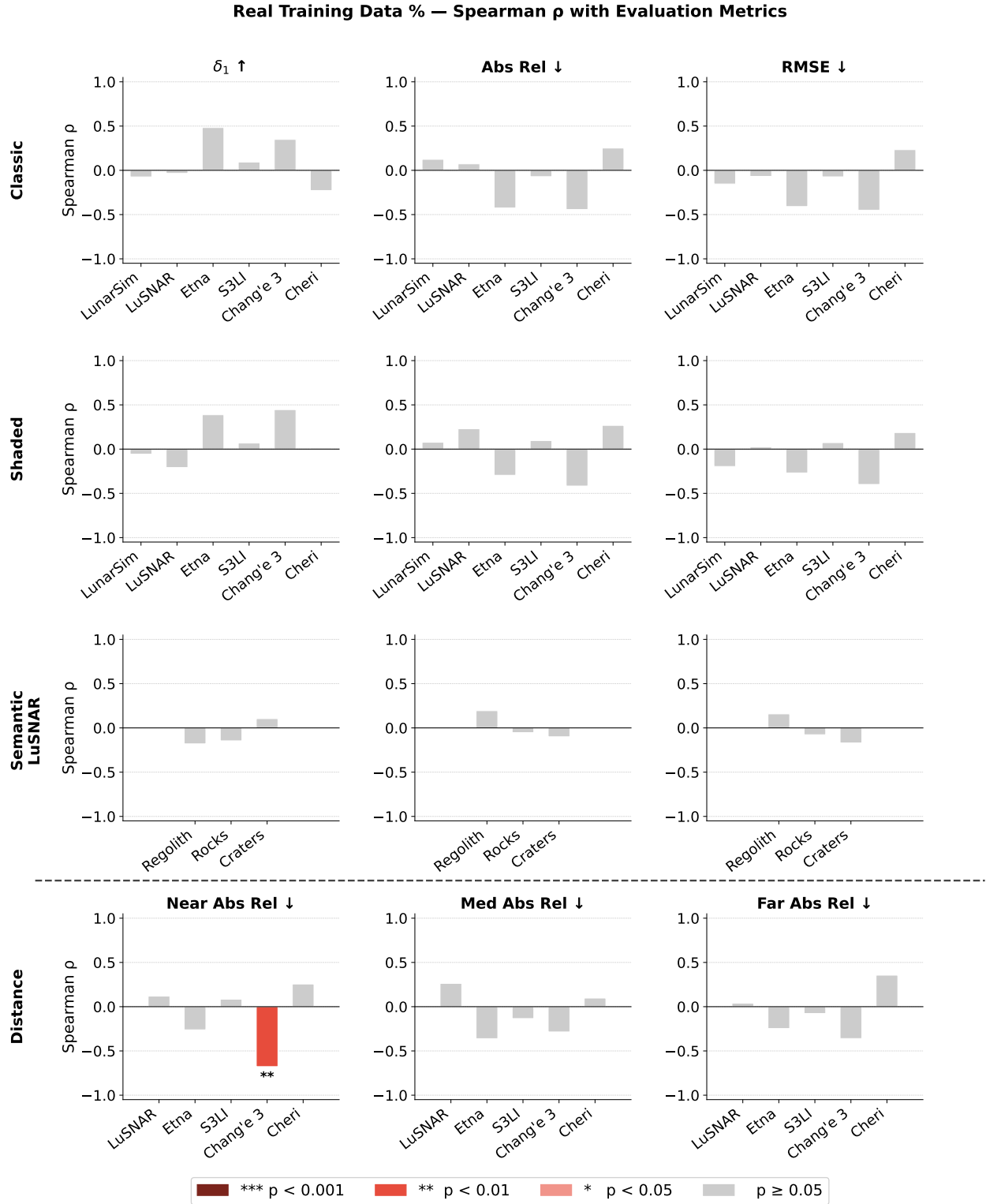


Figure S2. Spearman rank correlation (ρ) between the percentage of Real Training Data Percentage and evaluation metrics. This figure illustrates the correlation of the proportion of real-world training data with depth estimation performance (δ_1 , Abs Rel, RMSE) across standard dataset evaluations (Classic), extreme lighting conditions (Shaded), specific geological features (Semantic LuSNAR: Regolith, Rocks, Craters), and varying depth intervals (Distance: Near, Medium, Far). Statistical significance is indicated by p-values

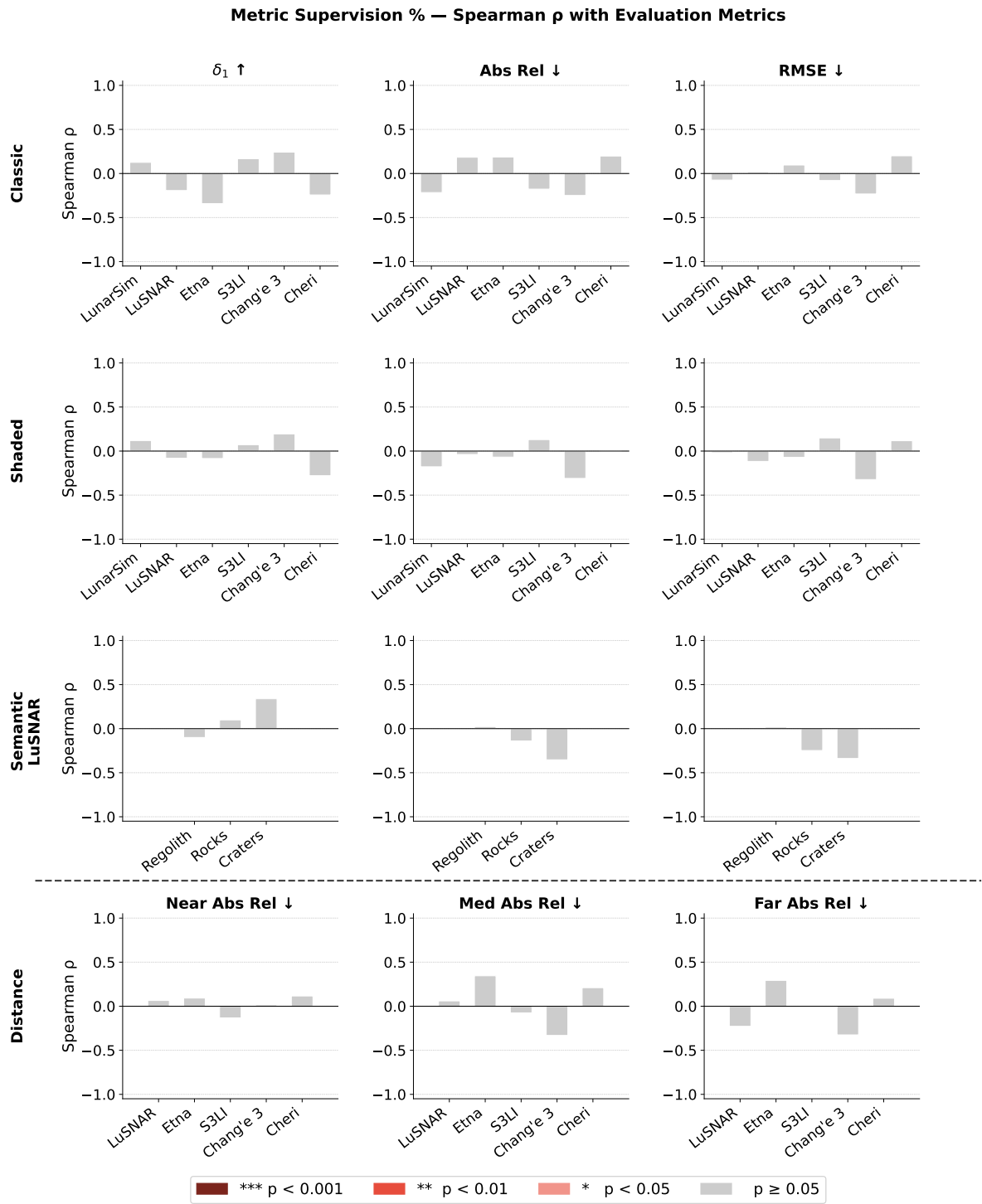


Figure S3. Spearman rank correlation (ρ) between the percentage of Metric Supervision and evaluation metrics. This plot illustrates the correlation of the proportion of metric supervision (percentage of the training data containing metric depth) used during training with depth estimation performance (δ_1 , Abs Rel, RMSE) across standard dataset evaluations (Classic), extreme lighting conditions (Shaded), specific geological features (Semantic LuSNAR: Regolith, Rocks, Craters), and varying depth intervals (Distance: Near, Medium, Far). Statistical significance is indicated by p-values.

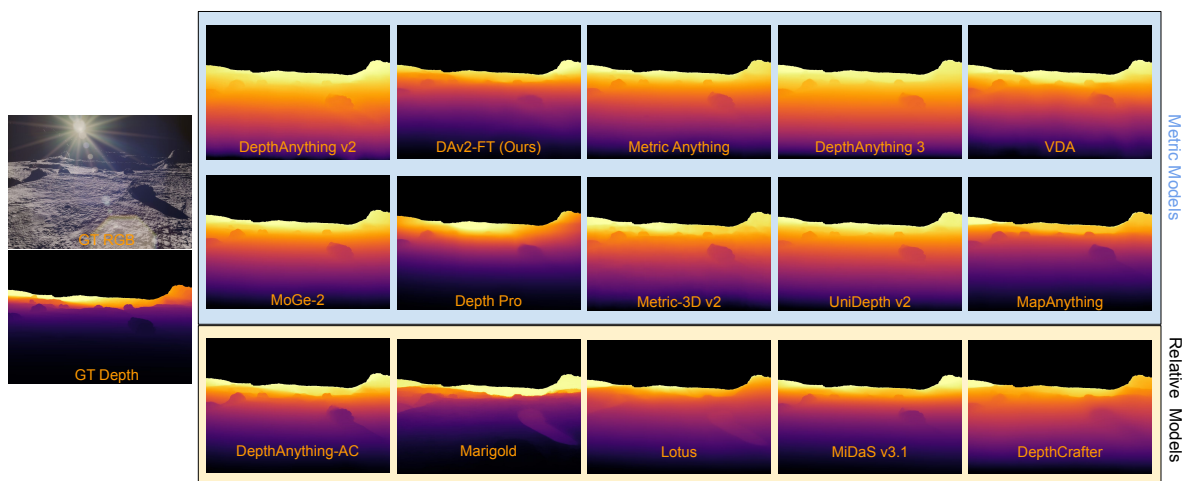


Figure S4. Qualitative depth estimation results on LunarSim

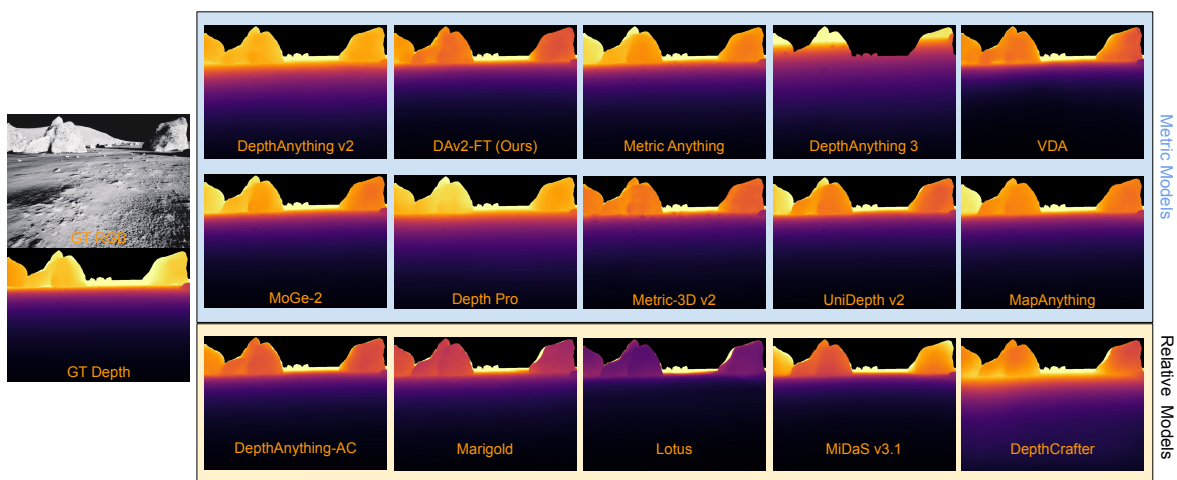


Figure S5. Qualitative depth estimation results on LuSNAR

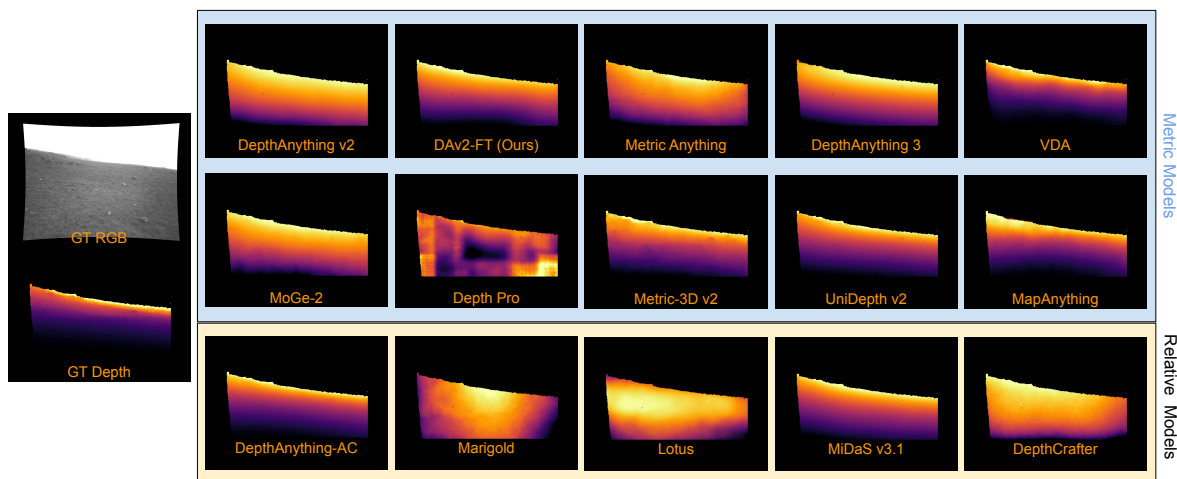


Figure S6. Qualitative depth estimation results on Etna-LRNT

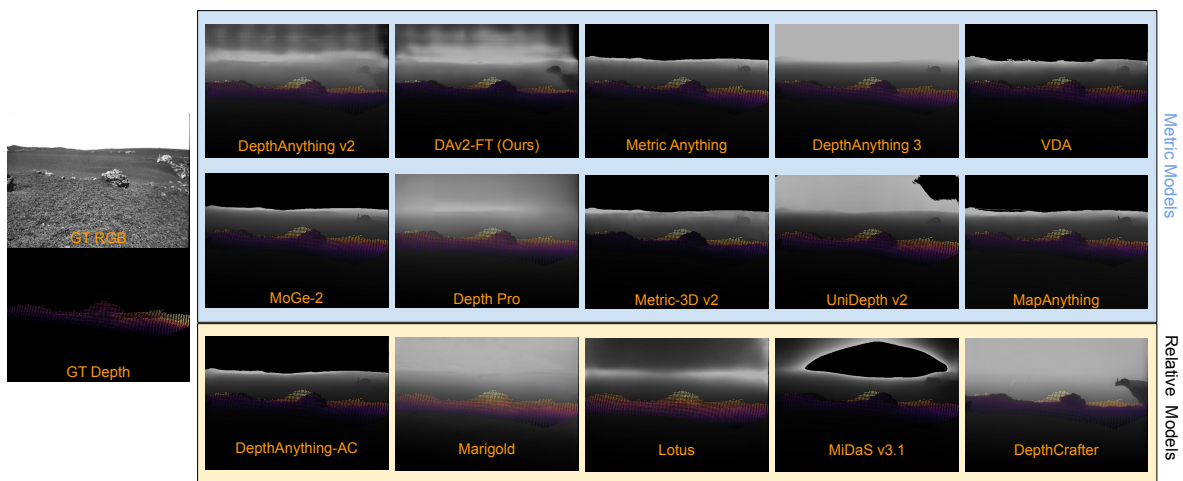


Figure S7. Qualitative depth estimation results on Etna-S3LI

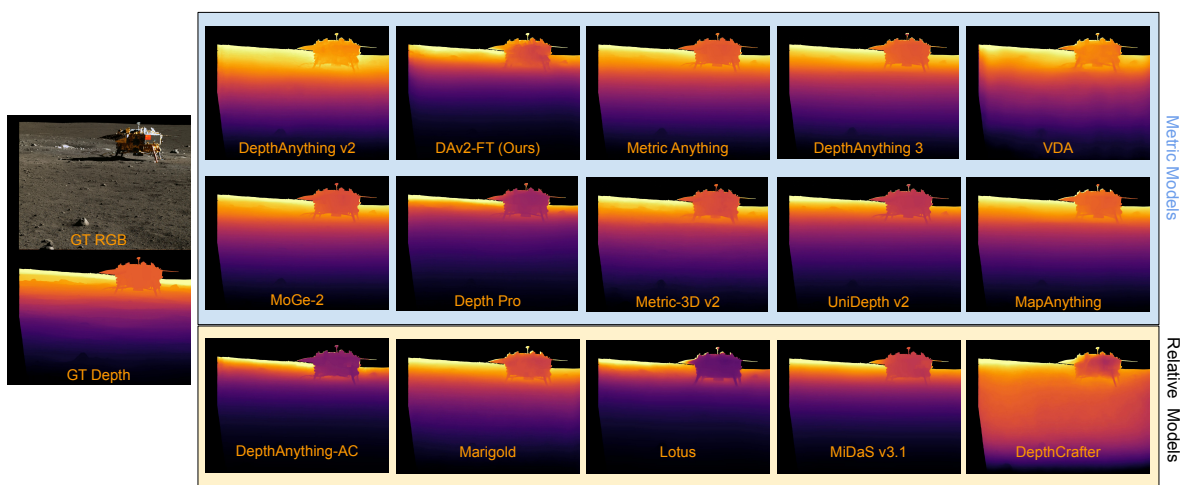


Figure S8. Qualitative depth estimation results on Chang'e-3

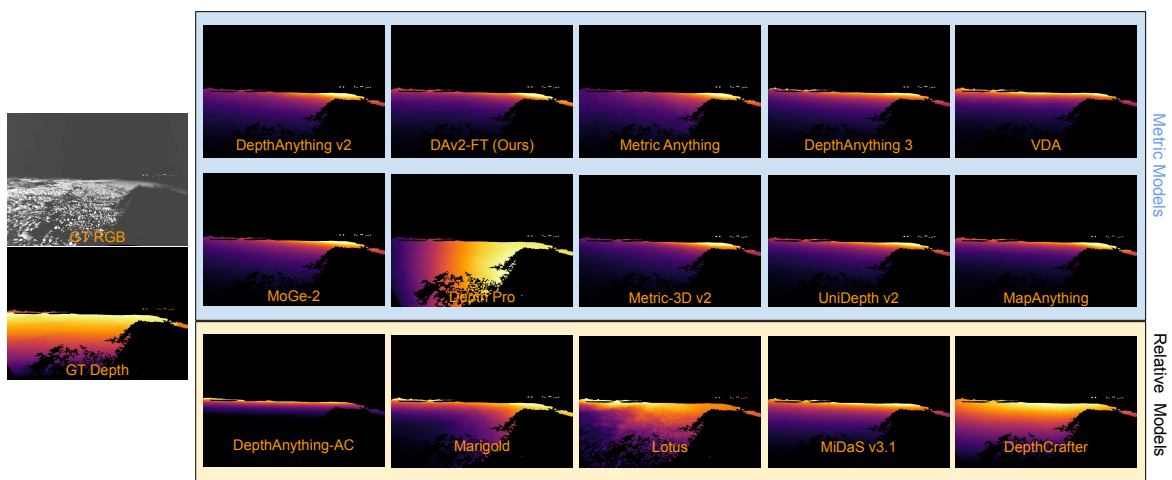


Figure S9. Qualitative depth estimation results on CHERI